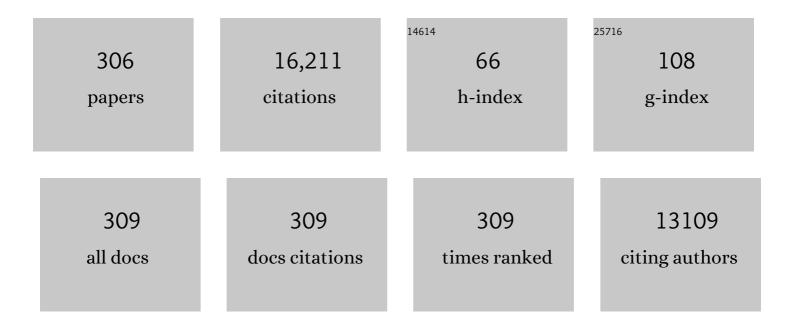
List of Publications by Year in descending order

Source: https://exaly.com/author-pdf/5639185/publications.pdf Version: 2024-02-01



| # | Article | IF | CITATIONS |
|----|--|------|-----------|
| 1 | Competing esterification and oligomerization reactions of typical long-chain alcohols to secondary organic aerosol formation. Journal of Environmental Sciences, 2023, 126, 103-112. | 3.2 | 1 |
| 2 | Photocatalytic mechanisms and photocatalyst deactivation during the degradation of 5-fluorouracil in water. Catalysis Today, 2023, 410, 45-55. | 2.2 | 6 |
| 3 | Persistence and environmental geochemistry transformation of antibiotic-resistance bacteria/genes in water at the interface of natural minerals with light irradiation. Critical Reviews in Environmental Science and Technology, 2022, 52, 2270-2301. | 6.6 | 9 |
| 4 | Formation mechanisms of viable but nonculturable bacteria through induction by light-based disinfection and their antibiotic resistance gene transfer risk: A review. Critical Reviews in Environmental Science and Technology, 2022, 52, 3651-3688. | 6.6 | 34 |
| 5 | Remediation of preservative ethylparaben in water using natural sphalerite: Kinetics and mechanisms. Journal of Environmental Sciences, 2022, 113, 72-80. | 3.2 | 5 |
| 6 | Highly efficient adsorption and catalytic degradation of ciprofloxacin by a novel heterogeneous Fenton catalyst of hexapod-like pyrite nanosheets mineral clusters. Applied Catalysis B: Environmental, 2022, 300, 120734. | 10.8 | 137 |
| 7 | Pollution profiles and human health risk assessment of atmospheric organophosphorus esters in an e-waste dismantling park and its surrounding area. Science of the Total Environment, 2022, 806, 151206. | 3.9 | 21 |
| 8 | Highly efficient removal of Cr(VI) by hexapod-like pyrite nanosheet clusters. Journal of Hazardous Materials, 2022, 424, 127504. | 6.5 | 19 |
| 9 | New advance in the application of compound-specific isotope analysis (CSIA) in identifying sources, transformation mechanisms and metabolism of brominated organic compounds. Critical Reviews in Environmental Science and Technology, 2022, 52, 3973-3996. | 6.6 | 3 |
| 10 | Occurrence and fate of polycyclic aromatic hydrocarbons from electronic waste dismantling activities: A critical review from environmental pollution to human health. Journal of Hazardous Materials, 2022, 424, 127683. | 6.5 | 28 |
| 11 | Adsorption and desorption mechanism of aromatic VOCs onto porous carbon adsorbents for emission control and resource recovery: recent progress and challenges. Environmental Science: Nano, 2022, 9, 81-104. | 2.2 | 35 |
| 12 | Atomic-level insight into effect of substrate concentration and relative humidity on photocatalytic degradation mechanism of gaseous styrene. Chemosphere, 2022, 291, 133074. | 4.2 | 2 |
| 13 | Urinary monohydroxylated polycyclic aromatic hydrocarbons in the general population from 26 provincial capital cities in China: Levels, influencing factors, and health risks. Environment International, 2022, 160, 107074. | 4.8 | 22 |
| 14 | Insight into phototransformation mechanism and toxicity evolution of novel and legacy brominated flame retardants in water: A comparative analysis. Water Research, 2022, 211, 118041. | 5.3 | 12 |
| 15 | Contribution of reaction of atmospheric amine with sulfuric acid to mixing particle formation from clay mineral. Science of the Total Environment, 2022, 821, 153336. | 3.9 | 2 |
| 16 | The stress response mechanisms of biofilm formation under sub-lethal photocatalysis. Applied Catalysis B: Environmental, 2022, 307, 121200. | 10.8 | 24 |
| 17 | Near-infrared light induced adsorption–desorption cycle for VOC recovery by integration of metal–organic frameworks with graphene oxide nanosheets. Environmental Science: Nano, 2022, 9, 1858-1868. | 2.2 | 11 |
| 18 | A new method of simultaneous determination of atmospheric amines in gaseous and particulate phases by gas chromatography-mass spectrometry. Journal of Environmental Sciences, 2022, 114, 401-411. | 3.2 | 5 |

| # | Article | IF | CITATIONS |
|----|--|------|-----------|
| 19 | Response mechanisms of different antibiotic-resistant bacteria with different resistance action targets to the stress from photocatalytic oxidation. Water Research, 2022, 218, 118407. | 5.3 | 28 |
| 20 | Potent necrosis effect of methanethiol mediated by METTL7B enzyme bioactivation mechanism in 16HBE cell. Ecotoxicology and Environmental Safety, 2022, 236, 113486. | 2.9 | 4 |
| 21 | Photoelectrocatalytic inactivation mechanism of E. coli DH5α (TET) and synergistic degradation of corresponding antibiotics in water. Water Research, 2022, 215, 118240. | 5.3 | 38 |
| 22 | Enhanced catalytic elimination of typical VOCs over ZnCoOx catalyst derived from in situ pyrolysis of ZnCo bimetallic zeolitic imidazolate frameworks. Applied Catalysis B: Environmental, 2022, 308, 121212. | 10.8 | 47 |
| 23 | How Does Vegetable Waste Decomposition Influence the Antibiotic Resistome and the Human Bacterial Pathogen Structure in Leachates?. ACS ES&T Water, 2022, 2, 226-236. | 2.3 | 10 |
| 24 | Levels and health risks of urinary phthalate metabolites and the association between phthalate exposure and unexplained recurrent spontaneous abortion: a large case-control study from China. Environmental Research, 2022, 212, 113393. | 3.7 | 10 |
| 25 | National-scale urinary phthalate metabolites in the general urban residents involving 26 provincial capital cities in China and the influencing factors as well as non-carcinogenic risks. Science of the Total Environment, 2022, 838, 156062. | 3.9 | 4 |
| 26 | The respiratory cytotoxicity of typical organophosphorus flame retardants on five different respiratory tract cells: Which are the most sensitive one?. Environmental Pollution, 2022, 307, 119564. | 3.7 | 11 |
| 27 | Elucidating the critical oligomeric steps in secondary organic aerosol and brown carbon formation. Atmospheric Chemistry and Physics, 2022, 22, 7259-7271. | 1.9 | 7 |
| 28 | Human exposure to BTEX emitted from a typical e-waste recycling industrial park: External and internal exposure levels, sources, and probabilistic risk implications. Journal of Hazardous Materials, 2022, 437, 129343. | 6.5 | 13 |
| 29 | Preferential removal of aromatics-dominated electronic industrial emissions using the integration of spray tower and photocatalysis technologies. Journal of Cleaner Production, 2022, 364, 132706. | 4.6 | 6 |
| 30 | Sub-lethal photocatalysis promotes horizontal transfer of antibiotic resistance genes by conjugation and transformability. Water Research, 2022, 221, 118808. | 5.3 | 15 |
| 31 | Atmospheric occurrences of nitrated and hydroxylated polycyclic aromatic hydrocarbons from typical e-waste dismantling sites. Environmental Pollution, 2022, 308, 119713. | 3.7 | 5 |
| 32 | Composition profiles of halogenated flame-retardants in the surface soils and in-situ cypress leaves from two chemical industrial parks. Science of the Total Environment, 2022, 845, 157129. | 3.9 | 0 |
| 33 | Increased adverse effects during metabolic transformation of short-chain chlorinated paraffins by cytochrome P450: A theoretical insight into 1-chlorodecane. Journal of Hazardous Materials, 2021, 407, 124391. | 6.5 | 14 |
| 34 | Recent advances in VOC elimination by catalytic oxidation technology onto various nanoparticles catalysts: a critical review. Applied Catalysis B: Environmental, 2021, 281, 119447. | 10.8 | 467 |
| 35 | Co-exposure and health risks of parabens, bisphenols, triclosan, phthalate metabolites and hydroxyl polycyclic aromatic hydrocarbons based on simultaneous detection in urine samples from guangzhou, south China. Environmental Pollution, 2021, 272, 115990. | 3.7 | 44 |
| 36 | Mechanisms of transplacental transport and barrier of polybrominated diphenyl ethers: A comprehensive human, Sprague-Dawley rat, BeWo cell and molecular docking study. Environmental Pollution, 2021, 270, 116091. | 3.7 | 2 |

| # | Article | IF | CITATIONS |
|----|--|------|-----------|
| 37 | Manipulation of plasmon-induced hot electron transport in Pd/MoO3-x@ZIF-8: Boosting the activity of Pd-catalyzed nitroaromatic hydrogenation under visible-light irradiation. Applied Catalysis B: Environmental, 2021, 282, 119511. | 10.8 | 29 |
| 38 | Occurrence and distribution of typical semi-volatile organic chemicals (SVOCs) in paired indoor and outdoor atmospheric fine particle samples from cities in southern China. Environmental Pollution, 2021, 269, 116123. | 3.7 | 19 |
| 39 | A review on in-vitro oral bioaccessibility of organic pollutants and its application in human exposure assessment. Science of the Total Environment, 2021, 752, 142001. | 3.9 | 26 |
| 40 | Boosting the photocatalytic degradation of ethyl acetate by a Z-scheme Au–TiO ₂ @NH ₂ -UiO-66 heterojunction with ultrafine Au as an electron mediator. Environmental Science: Nano, 2021, 8, 2542-2553. | 2.2 | 21 |
| 41 | Pollution profile of waterborne bacterial and fungal community in urban Rivers of Pearl River estuary: Microbial safety assessment. Journal of Freshwater Ecology, 2021, 36, 305-322. | 0.5 | 2 |
| 42 | Photochemical degradation of fragrance ingredient benzyl formate in water: Mechanism and toxicity assessment. Ecotoxicology and Environmental Safety, 2021, 211, 111950. | 2.9 | 11 |
| 43 | Highly efficient and selective photoreduction of CO2 to CO with nanosheet g-C3N4 as compared with its bulk counterpart. Environmental Research, 2021, 195, 110880. | 3.7 | 30 |
| 44 | Superoxide radical enhanced photocatalytic performance of styrene alters its degradation mechanism and intermediate health risk on TiO2/graphene surface. Environmental Research, 2021, 195, 110747. | 3.7 | 27 |
| 45 | Formation kinetics and mechanisms of ozone and secondary organic aerosols from photochemical oxidation of different aromatic hydrocarbons: dependence on NO _{<i>x</i>} and organic substituents. Atmospheric Chemistry and Physics. 2021, 21, 7567-7578. | 1.9 | 14 |
| 46 | Visible Light-Induced Marine Bacterial Inactivation in Seawater by an <i>In Situ</i> Photo-Fenton System without Additional Oxidants: Implications for Ballast Water Sterilization. ACS ES&T Water, 2021, 1, 1483-1494. | 2.3 | 45 |
| 47 | Traditional and Emerging Water Disinfection Technologies Challenging the Control of Antibiotic-Resistant Bacteria and Antibiotic Resistance Genes. ACS ES&T Engineering, 2021, 1, 1046-1064. | 3.7 | 66 |
| 48 | Can photocatalytic technology facilitate conjugative transfer of ARGs in bacteria at the interface of natural sphalerite under different light irradiation?. Applied Catalysis B: Environmental, 2021, 287, 119977. | 10.8 | 30 |
| 49 | A critical review on human internal exposure of phthalate metabolites and the associated health risks. Environmental Pollution, 2021, 279, 116941. | 3.7 | 77 |
| 50 | Assessing the role of mineral particles in the atmospheric photooxidation of typical carbonyl compound. Journal of Environmental Sciences, 2021, 105, 56-63. | 3.2 | 3 |
| 51 | Photocatalytic inactivation and destruction of harmful microalgae Karenia mikimotoi under visible-light irradiation: Insights into physiological response and toxicity assessment. Environmental Research, 2021, 198, 111295. | 3.7 | 25 |
| 52 | Volatile organic compounds in an e-waste dismantling region: From spatial-seasonal variation to human health impact. Chemosphere, 2021, 275, 130022. | 4.2 | 42 |
| 53 | Low concentration Tetrabromobisphenol A (TBBPA) elevating overall metabolism by inducing activation of the Ras signaling pathway. Journal of Hazardous Materials, 2021, 416, 125797. | 6.5 | 26 |
| 54 | In vitro toxic synergistic effects of exogenous pollutants-trimethylamine and its metabolites on human respiratory tract cells. Science of the Total Environment, 2021, 783, 146915. | 3.9 | 20 |

| # | Article | IF | CITATIONS |
|----|---|------|-----------|
| 55 | Insights into the Photodegradation of the Contact Allergen Fragrance Cinnamyl Alcohol: Kinetics, Mechanism, and Toxicity. Environmental Toxicology and Chemistry, 2021, 40, 2705-2714. | 2.2 | 0 |
| 56 | PAHs and their hydroxylated metabolites in the human fingernails from e-waste dismantlers: Implications for human non-invasive biomonitoring and exposure. Environmental Pollution, 2021, 283, 117059. | 3.7 | 18 |
| 57 | Contributions of meat waste decomposition to the abundance and diversity of pathogens and antibiotic-resistance genes in the atmosphere. Science of the Total Environment, 2021, 784, 147128. | 3.9 | 27 |
| 58 | An inescapable fact: Toxicity increase during photo-driven degradation of emerging contaminants in water environments. Current Opinion in Green and Sustainable Chemistry, 2021, 30, 100472. | 3.2 | 3 |
| 59 | Human exposome and biomarker database for soil pollutants at typical sites of industrial contamination. Science Bulletin, 2021, 66, 1705-1708. | 4.3 | 3 |
| 60 | Pollution profiles, removal performance and health risk reduction of malodorous volatile organic compounds emitted from municipal leachate treating process. Journal of Cleaner Production, 2021, 315, 128141. | 4.6 | 12 |
| 61 | Fouling of TiO2 induced by natural organic matters during photocatalytic water treatment: Mechanisms and regeneration strategy. Applied Catalysis B: Environmental, 2021, 294, 120252. | 10.8 | 60 |
| 62 | Identifying Dermal Uptake as a Significant Pathway for Human Exposure to Typical Semivolatile Organic Compounds in an E-Waste Dismantling Site: The Relationship of Contaminant Levels in Handwipes and Urine Metabolites. Environmental Science & Technology, 2021, 55, 14026-14036. | 4.6 | 33 |
| 63 | The exposures and health effects of benzene, toluene and naphthalene for Chinese chefs in multiple cooking styles of kitchens. Environment International, 2021, 156, 106721. | 4.8 | 33 |
| 64 | Metagenomic profiles and health risks of pathogens and antibiotic resistance genes in various industrial wastewaters and the associated receiving surface water. Chemosphere, 2021, 283, 131224. | 4.2 | 39 |
| 65 | Organophosphate flame retardants, tetrabromobisphenol A, and their transformation products in sediment of e-waste dismantling areas and the flame-retardant production base. Ecotoxicology and Environmental Safety, 2021, 225, 112717. | 2.9 | 15 |
| 66 | Solar-light-triggered regenerative adsorption removal of styrene by silver nanoparticles incorporated in metal–organic frameworks. Environmental Science: Nano, 2021, 8, 543-553. | 2.2 | 16 |
| 67 | Mechanism for Rapid Conversion of Amines to Ammonium Salts at the Air–Particle Interface. Journal of the American Chemical Society, 2021, 143, 1171-1178. | 6.6 | 19 |
| 68 | Atomically dispersed Pd sites on Ti-SBA-15 for efficient catalytic combustion of typical gaseous VOCs. Environmental Science: Nano, 2021, 8, 3735-3745. | 2.2 | 11 |
| 69 | Advances in ecological and health risks of biochar during environmental applications. Chinese Science Bulletin, 2021, 66, 5-20. | 0.4 | 4 |
| 70 | Insights into biomonitoring of human exposure to polycyclic aromatic hydrocarbons with hair analysis: A case study in e-waste recycling area. Environment International, 2020, 136, 105432. | 4.8 | 35 |
| 71 | A new advance in the potential exposure to "old―and "new―halogenated flame retardants in the atmospheric environments and biota: From occurrence to transformation products and metabolites. Critical Reviews in Environmental Science and Technology, 2020, 50, 1935-1983. | 6.6 | 17 |
| 72 | Removal of volatile organic compounds (VOCs) emitted from a textile dyeing wastewater treatment plant and the attenuation of respiratory health risks using a pilot-scale biofilter. Journal of Cleaner Production, 2020, 253, 120019. | 4.6 | 66 |

| # | Article | IF | CITATIONS |
|----|--|------|-----------|
| 73 | Few-layered tungsten selenide as a co-catalyst for visible-light-driven photocatalytic production of hydrogen peroxide for bacterial inactivation. Environmental Science: Nano, 2020, 7, 3877-3887. | 2.2 | 26 |
| 74 | Field study of PAHs with their derivatives emitted from e-waste dismantling processes and their comprehensive human exposure implications. Environment International, 2020, 144, 106059. | 4.8 | 34 |
| 75 | Temporal trends of "old―and "new―persistent halogenated organic pollutants in fish from the third largest freshwater lake in China during 2011–2018 and the associated health risks. Environmental Pollution, 2020, 267, 115497. | 3.7 | 24 |
| 76 | Atmospheric diffusion profiles and health risks of typical VOC: Numerical modelling study. Journal of Cleaner Production, 2020, 275, 122982. | 4.6 | 54 |
| 77 | Mechanism of atmospheric organic amines reacted with ozone and implications for the formation of secondary organic aerosols. Science of the Total Environment, 2020, 737, 139830. | 3.9 | 23 |
| 78 | Mechanism investigation and stable isotope change during photochemical degradation of tetrabromobisphenol A (TBBPA) in water under LED white light irradiation. Chemosphere, 2020, 258, 127378. | 4.2 | 13 |
| 79 | Carbenium ion-mediated oligomerization of methylglyoxal for secondary organic aerosol formation. Proceedings of the National Academy of Sciences of the United States of America, 2020, 117, 13294-13299. | 3.3 | 28 |
| 80 | Enhanced H-abstraction contribution for oxidation of xylenes via mineral particles: Implications for particulate matter formation and human health. Environmental Research, 2020, 186, 109568. | 3.7 | 16 |
| 81 | Reactor characterization and primary application of a state of art dual-reactor chamber in the investigation of atmospheric photochemical processes. Journal of Environmental Sciences, 2020, 98, 161-168. | 3.2 | 11 |
| 82 | Enhanced uptake of glyoxal at the acidic nanoparticle interface: implications for secondary organic aerosol formation. Environmental Science: Nano, 2020, 7, 1126-1135. | 2.2 | 16 |
| 83 | Mechanism of the atmospheric chemical transformation of acetylacetone and its implications in night-time second organic aerosol formation. Science of the Total Environment, 2020, 720, 137610. | 3.9 | 9 |
| 84 | Pollution profiles of antibiotic resistance genes associated with airborne opportunistic pathogens from typical area, Pearl River Estuary and their exposure risk to human. Environment International, 2020, 143, 105934. | 4.8 | 70 |
| 85 | Malodorous gases production from food wastes decomposition by indigenous microorganisms. Science of the Total Environment, 2020, 717, 137175. | 3.9 | 36 |
| 86 | Accelerated evolution of bacterial antibiotic resistance through early emerged stress responses driven by photocatalytic oxidation. Applied Catalysis B: Environmental, 2020, 269, 118829. | 10.8 | 55 |
| 87 | Introduce oxygen vacancies into CeO2 catalyst for enhanced coke resistance during photothermocatalytic oxidation of typical VOCs. Applied Catalysis B: Environmental, 2020, 269, 118755. | 10.8 | 184 |
| 88 | Natural sphalerite nanoparticles can accelerate horizontal transfer of plasmid-mediated antibiotic-resistance genes. Environment International, 2020, 136, 105497. | 4.8 | 66 |
| 89 | Bacterial response mechanism during biofilm growth on different metal material substrates: EPS characteristics, oxidative stress and molecular regulatory network analysis. Environmental Research, 2020, 185, 109451. | 3.7 | 50 |
| 90 | Visible light activation of persulfate by magnetic hydrochar for bacterial inactivation: Efficiency, recyclability and mechanisms. Water Research, 2020, 176, 115746. | 5.3 | 89 |

| # | Article | IF | CITATIONS |
|-----|--|------|-----------|
| 91 | Photocatalytic degradation mechanism of gaseous styrene over Au/TiO2@CNTs: Relevance of superficial state with deactivation mechanism. Applied Catalysis B: Environmental, 2020, 272, 118969. | 10.8 | 84 |
| 92 | <i>In situ</i> growth of well-aligned Ni-MOF nanosheets on nickel foam for enhanced photocatalytic degradation of typical volatile organic compounds. Nanoscale, 2020, 12, 9462-9470. | 2.8 | 66 |
| 93 | Unexpected culprit of increased estrogenic effects: Oligomers in the photodegradation of preservative ethylparaben in water. Water Research, 2020, 176, 115745. | 5.3 | 24 |
| 94 | The exposure risk of typical VOCs to the human beings via inhalation based on the respiratory deposition rates by proton transfer reaction-time of flight-mass spectrometer. Ecotoxicology and Environmental Safety, 2020, 197, 110615. | 2.9 | 23 |
| 95 | Halogenated and organophosphorous flame retardants in surface soils from an e-waste dismantling park and its surrounding area: Distributions, sources, and human health risks. Environment International, 2020, 139, 105741. | 4.8 | 73 |
| 96 | Simultaneous Determination of Multiple Classes of Phenolic Compounds in Human Urine: Insight into Metabolic Biomarkers of Occupational Exposure to E-Waste. Environmental Science and Technology Letters, 2020, 7, 323-329. | 3.9 | 27 |
| 97 | Photocatalytic reductive defluorination of perfluorooctanoic acid in water under visible light irradiation: the role of electron donor. Environmental Science: Water Research and Technology, 2020, 6, 1638-1648. | 1.2 | 17 |
| 98 | A non-blue laccase of Bacillus sp. GZB displays manganese-oxidase activity: A study of laccase characterization, Mn(II) oxidation and prediction of Mn(II) oxidation mechanism. Chemosphere, 2020, 252, 126619. | 4.2 | 12 |
| 99 | The pollution profiles and human exposure risks of chlorinated and brominated PAHs in indoor dusts from e-waste dismantling workshops: Comparison of GC–MS, GC–MS/MS and GC × GC–MS/MS determination methods. Journal of Hazardous Materials, 2020, 394, 122573. | 6.5 | 36 |
| 100 | Spatial and temporal distribution characteristics and ozone formation potentials of volatile organic compounds from three typical functional areas in China. Environmental Research, 2020, 183, 109141. | 3.7 | 34 |
| 101 | The formation mechanism of antibiotic-resistance genes associated with bacterial communities during biological decomposition of household garbage. Journal of Hazardous Materials, 2020, 398, 122973. | 6.5 | 31 |
| 102 | Microwave-assisted synthesis of defective tungsten trioxide for photocatalytic bacterial inactivation: Role of the oxygen vacancy. Chinese Journal of Catalysis, 2020, 41, 1488-1497. | 6.9 | 27 |
| 103 | In-situ decoration of metallic Bi on BiOBr with exposed (110) facets and surface oxygen vacancy for enhanced solar light photocatalytic degradation of gaseous n-hexane. Chinese Journal of Catalysis, 2020, 41, 1603-1612. | 6.9 | 78 |
| 104 | Toxicity mechanism of tetrabromobisphenol A to human respiratory system cells 16HBE and Beas2B. Chinese Science Bulletin, 2020, 65, 931-939. | 0.4 | 2 |
| 105 | Cutting down on the ozone and SOA formation as well as health risks of VOCs emitted from e-waste dismantlement by integration technique. Journal of Environmental Management, 2019, 249, 107755. | 3.8 | 22 |
| 106 | Pollution profiles of volatile organic compounds from different urban functional areas in Guangzhou China based on GC/MS and PTR-TOF-MS: Atmospheric environmental implications. Atmospheric Environment, 2019, 214, 116843. | 1.9 | 52 |
| 107 | OH radicals determined photocatalytic degradation mechanisms of gaseous styrene in TiO2 system under 254 nm versus 185 nm irradiation: Combined experimental and theoretical studies. Applied Catalysis B: Environmental, 2019, 257, 117912. | 10.8 | 84 |
| 108 | The heterogeneous reaction of dimethylamine/ammonia with sulfuric acid to promote the growth of atmospheric nanoparticles. Environmental Science: Nano, 2019, 6, 2767-2776. | 2.2 | 9 |

| # | Article | IF | CITATIONS |
|-----|---|------|-----------|
| 109 | Purification, molecular characterization and metabolic mechanism of an aerobic tetrabromobisphenol A dehalogenase, a key enzyme of halorespiration in Ochrobactrum sp. T. Chemosphere, 2019, 237, 124461. | 4.2 | 11 |
| 110 | Activation of NF-κB pathways mediating the inflammation and pulmonary diseases associated with atmospheric methylamine exposure. Environmental Pollution, 2019, 252, 1216-1224. | 3.7 | 21 |
| 111 | Biodegradation of typical BFRs 2,4,6-tribromophenol by an indigenous strain Bacillus sp. GZT isolated from e-waste dismantling area through functional heterologous expression. Science of the Total Environment, 2019, 697, 134159. | 3.9 | 10 |
| 112 | Pollution evaluation and health risk assessment of airborne toxic metals in both indoors and outdoors of the Pearl River Delta, China. Environmental Research, 2019, 179, 108793. | 3.7 | 28 |
| 113 | Sub-lethal photocatalysis bactericidal technology cause longer persistence of antibiotic-resistance mutant and plasmid through the mechanism of reduced fitness cost. Applied Catalysis B: Environmental, 2019, 245, 698-705. | 10.8 | 24 |
| 114 | Micro/nano-bubble assisted synthesis of Au/TiO ₂ @CNTs composite photocatalyst for photocatalytic degradation of gaseous styrene and its enhanced catalytic mechanism. Environmental Science: Nano, 2019, 6, 948-958. | 2.2 | 62 |
| 115 | Photochemical degradation kinetics and mechanism of short-chain chlorinated paraffins in aqueous solution: A case of 1-chlorodecane. Environmental Pollution, 2019, 247, 362-370. | 3.7 | 23 |
| 116 | Photocatalytic ozonation mechanism of gaseous <i>n</i> -hexane on MO _x –TiO ₂ –foam nickel composite (M = Cu, Mn, Ag): unveiling the role of ˙OH and Ë™O ₂ ^{â^'} . Environmental Science: Nano, 2019, 6, 959-969. | 2.2 | 46 |
| 117 | New theoretical insight into indirect photochemical transformation of fragrance nitro-musks: Mechanisms, eco-toxicity and health effects. Environment International, 2019, 129, 68-75. | 4.8 | 64 |
| 118 | Release of tetrabromobisphenol A (TBBPA)-derived non-extractable residues in oxic soil and the effects of the TBBPA-degrading bacterium Ochrobactrum sp. strain T. Journal of Hazardous Materials, 2019, 378, 120666. | 6.5 | 15 |
| 119 | Solar light induced transformation mechanism of allyl alcohol to monocarbonyl and dicarbonyl compounds on different TiO2: A combined experimental and theoretical investigation. Chemosphere, 2019, 232, 287-295. | 4.2 | 11 |
| 120 | Seasonal profiles of atmospheric PAHs in an e-waste dismantling area and their associated health risk considering bioaccessible PAHs in the human lung. Science of the Total Environment, 2019, 683, 371-379. | 3.9 | 44 |
| 121 | Density functional theory investigation of the enhanced adsorption mechanism and potential catalytic activity for formaldehyde degradation on Al-decorated C2N monolayer. Chinese Journal of Catalysis, 2019, 40, 664-672. | 6.9 | 44 |
| 122 | The mixing state of mineral dusts with typical anthropogenic pollutants: A mechanism study. Atmospheric Environment, 2019, 209, 192-200. | 1.9 | 7 |
| 123 | Silver sulfide nanoparticles in aqueous environments: formation, transformation and toxicity. Environmental Science: Nano, 2019, 6, 1674-1687. | 2.2 | 35 |
| 124 | Photocatalytic defluorination of perfluorooctanoic acid by surface defective BiOCl: Fast microwave solvothermal synthesis and photocatalytic mechanisms. Journal of Environmental Sciences, 2019, 84, 69-79. | 3.2 | 30 |
| 125 | Highly efficient visible-light-driven photocatalytic degradation of VOCs by CO2-assisted synthesized mesoporous carbon confined mixed-phase TiO2 nanocomposites derived from MOFs. Applied Catalysis B: Environmental, 2019, 250, 337-346. | 10.8 | 113 |
| 126 | Catalyst-free activation of persulfate by visible light for water disinfection: Efficiency and mechanisms. Water Research, 2019, 157, 106-118. | 5.3 | 145 |

| # | Article | IF | CITATIONS |
|-----|--|------|-----------|
| 127 | Metal–organic framework-based nanomaterials for adsorption and photocatalytic degradation of gaseous pollutants: recent progress and challenges. Environmental Science: Nano, 2019, 6, 1006-1025. | 2.2 | 245 |
| 128 | Comparing pollution patterns and human exposure to atmospheric PBDEs and PCBs emitted from different e-waste dismantling processes. Journal of Hazardous Materials, 2019, 369, 142-149. | 6.5 | 58 |
| 129 | Genome sequence of a spore-laccase forming, BPA-degrading Bacillus sp. GZB isolated from an electronic-waste recycling site reveals insights into BPA degradation pathways. Archives of Microbiology, 2019, 201, 623-638. | 1.0 | 15 |
| 130 | Simultaneous determination of polybrominated diphenyl ethers, polycyclic aromatic hydrocarbons and their hydroxylated metabolites in human hair: a potential methodology to distinguish external from internal exposure. Analyst, The, 2019, 144, 7227-7235. | 1.7 | 24 |
| 131 | Chlorinated paraffins in the indoor and outdoor atmospheric particles from the Pearl River Delta: Characteristics, sources, and human exposure risks. Science of the Total Environment, 2019, 650, 1041-1049. | 3.9 | 41 |
| 132 | Relationships between the bioavailability of polybrominated diphenyl ethers in soils measured with female C57BL/6 mice and the bioaccessibility determined using five in vitro methods. Environment International, 2019, 123, 337-344. | 4.8 | 27 |
| 133 | Application of a novel gene encoding bromophenol dehalogenase from Ochrobactrum sp. T in TBBPA degradation. Chemosphere, 2019, 217, 507-515. | 4.2 | 30 |
| 134 | Protocatechuic acid promoted catalytic degradation of rhodamine B with Fe@Fe2O3 core-shell nanowires by molecular oxygen activation mechanism. Catalysis Today, 2019, 335, 144-150. | 2.2 | 17 |
| 135 | Antibiotic-resistance gene transfer in antibiotic-resistance bacteria under different light irradiation: Implications from oxidative stress and gene expression. Water Research, 2019, 149, 282-291. | 5.3 | 115 |
| 136 | The synergic degradation mechanism and photothermocatalytic mineralization of typical VOCs over PtCu/CeO2 ordered porous catalysts under simulated solar irradiation. Journal of Catalysis, 2019, 370, 88-96. | 3.1 | 69 |
| 137 | Enhanced photocatalytic mechanism of Ag3PO4 nano-sheets using MS2 (M = Mo, W)/rGO hybrids as co-catalysts for 4-nitrophenol degradation in water. Applied Catalysis B: Environmental, 2018, 232, 11-18. | 10.8 | 75 |
| 138 | Persistent free radicals in carbon-based materials on transformation of refractory organic contaminants (ROCs) in water: A critical review. Water Research, 2018, 137, 130-143. | 5.3 | 255 |
| 139 | Adsorption mechanisms of different volatile organic compounds onto pristine C2N and Al-doped C2N monolayer: A DFT investigation. Applied Surface Science, 2018, 450, 484-491. | 3.1 | 90 |
| 140 | Free-standing red phosphorous/silver sponge monolith as an efficient and easily recyclable macroscale photocatalyst for organic pollutant degradation under visible light irradiation. Journal of Colloid and Interface Science, 2018, 518, 130-139. | 5.0 | 30 |
| 141 | Antibiotics elimination and risk reduction at two drinking water treatment plants by using different conventional treatment techniques. Ecotoxicology and Environmental Safety, 2018, 158, 154-161. | 2.9 | 31 |
| 142 | A coupled technique to eliminate overall nonpolar and polar volatile organic compounds from paint production industry. Journal of Cleaner Production, 2018, 185, 266-274. | 4.6 | 25 |
| 143 | Enhanced Visible-Light-Driven Photocatalytic Bacterial Inactivation by Ultrathin Carbon-Coated Magnetic Cobalt Ferrite Nanoparticles. Environmental Science & Technology, 2018, 52, 4774-4784. | 4.6 | 108 |
| 144 | Enhanced visible-light photocatalytic activity to volatile organic compounds degradation and deactivation resistance mechanism of titania confined inside a metal-organic framework. Journal of Colloid and Interface Science, 2018, 522, 174-182. | 5.0 | 81 |

| # | Article | IF | CITATIONS |
|-----|---|------|-----------|
| 145 | Spatial distributions, source apportionment and ecological risk of SVOCs in water and sediment from Xijiang River, Pearl River Delta. Environmental Geochemistry and Health, 2018, 40, 1853-1865. | 1.8 | 18 |
| 146 | Novel approach for removing brominated flame retardant from aquatic environments using Cu/Fe-based metal-organic frameworks: A case of hexabromocyclododecane (HBCD). Science of the Total Environment, 2018, 621, 1533-1541. | 3.9 | 61 |
| 147 | Delineation of 3D dose-time-toxicity in human pulmonary epithelial Beas-2B cells induced by decabromodiphenyl ether (BDE209). Environmental Pollution, 2018, 243, 661-669. | 3.7 | 21 |
| 148 | OH-Initiated Oxidation of Acetylacetone: Implications for Ozone and Secondary Organic Aerosol Formation. Environmental Science & amp; Technology, 2018, 52, 11169-11177. | 4.6 | 43 |
| 149 | Photocatalytic hydrogen evolution and bacterial inactivation utilizing sonochemical-synthesized g-C3N4/red phosphorus hybrid nanosheets as a wide-spectral-responsive photocatalyst: The role of type I band alignment. Applied Catalysis B: Environmental, 2018, 238, 126-135. | 10.8 | 209 |
| 150 | Novel inÂvitro method for measuring the mass fraction of bioaccessible atmospheric polycyclic aromatic hydrocarbons using simulated human lung fluids. Environmental Pollution, 2018, 242, 1633-1641. | 3.7 | 11 |
| 151 | Spore cells from BPA degrading bacteria Bacillus sp. GZB displaying high laccase activity and stability for BPA degradation. Science of the Total Environment, 2018, 640-641, 798-806. | 3.9 | 70 |
| 152 | Fabrication of Au/TiO 2 nanowires@carbon fiber paper ternary composite for visible-light photocatalytic degradation of gaseous styrene. Catalysis Today, 2017, 281, 621-629. | 2.2 | 45 |
| 153 | Influence of photoinduced Bi-related self-doping on the photocatalytic activity of BiOBr nanosheets. Applied Surface Science, 2017, 391, 516-524. | 3.1 | 58 |
| 154 | Using an integrated decontamination technique to remove VOCs and attenuate health risks from an e-waste dismantling workshop. Chemical Engineering Journal, 2017, 318, 57-63. | 6.6 | 47 |
| 155 | Activation of persulfates by natural magnetic pyrrhotite for water disinfection: Efficiency, mechanisms, and stability. Water Research, 2017, 112, 236-247. | 5.3 | 176 |
| 156 | Photocatalytic nanomaterials for solar-driven bacterial inactivation: recent progress and challenges. Environmental Science: Nano, 2017, 4, 782-799. | 2.2 | 239 |
| 157 | Preferential purification of oxygenated volatile organic compounds than monoaromatics emitted from paint spray booth and risk attenuation by the integrated decontamination technique. Journal of Cleaner Production, 2017, 148, 268-275. | 4.6 | 27 |
| 158 | Visible-light-enhanced photothermocatalytic activity of ABO3-type perovskites for the decontamination of gaseous styrene. Applied Catalysis B: Environmental, 2017, 209, 146-154. | 10.8 | 108 |
| 159 | Interaction between bacterial cell membranes and nano-TiO2 revealed by two-dimensional FTIR correlation spectroscopy using bacterial ghost as a model cell envelope. Water Research, 2017, 118, 104-113. | 5.3 | 48 |
| 160 | Enhanced photocatalytic inactivation of Escherichia coli by a novel Z-scheme g-C 3 N 4 /m-Bi 2 O 4 hybrid photocatalyst under visible light: The role of reactive oxygen species. Applied Catalysis B: Environmental, 2017, 214, 23-33. | 10.8 | 210 |
| 161 | Accelerated biodegradation of BPA in water-sediment microcosms with Bacillus sp. GZB and the associated bacterial community structure. Chemosphere, 2017, 184, 120-126. | 4.2 | 44 |
| 162 | Earth-abundant Ni2P/g-C3N4 lamellar nanohydrids for enhanced photocatalytic hydrogen evolution and bacterial inactivation under visible light irradiation. Applied Catalysis B: Environmental, 2017, 217, 570-580. | 10.8 | 311 |

| # | Article | IF | CITATIONS |
|-----|---|-----|-----------|
| 163 | Purifying, cloning and characterizing a novel dehalogenase from Bacillus sp. GZT to enhance the biodegradation of 2,4,6-tribromophenol in water. Environmental Pollution, 2017, 225, 104-111. | 3.7 | 16 |
| 164 | Photo-induced oxidative damage to dissolved free amino acids by the photosensitizer polycyclic musk tonalide: Transformation kinetics and mechanisms. Water Research, 2017, 115, 339-346. | 5.3 | 17 |
| 165 | Bacterial Oxidative Stress Responses and Cellular Damage Caused by Photocatalytic and Photoelectrocatalytic Inactivation. Green Chemistry and Sustainable Technology, 2017, , 259-272. | 0.4 | 2 |
| 166 | Probing the intracellular organic matters released from the photocatalytic inactivation of bacteria using fractionation procedure and excitation-emission-matrix fluorescence. Water Research, 2017, 110, 270-280. | 5.3 | 33 |
| 167 | Photocatalytic and Photoelectrocatalytic Inactivation Mechanism of Biohazards. Green Chemistry and Sustainable Technology, 2017, , 221-237. | 0.4 | 1 |
| 168 | Elimination of antibiotic-resistance bacterium and its associated/dissociative bla and aac(3)-II antibiotic-resistance genes in aqueous system via photoelectrocatalytic process. Water Research, 2017, 125, 219-226. | 5.3 | 67 |
| 169 | Natural magnetic pyrrhotite as a high-Efficient persulfate activator for micropollutants degradation: Radicals identification and toxicity evaluation. Journal of Hazardous Materials, 2017, 340, 435-444. | 6.5 | 81 |
| 170 | The evolution of pollution profile and health risk assessment for three groups SVOCs pollutants along with Beijiang River, China. Environmental Geochemistry and Health, 2017, 39, 1487-1499. | 1.8 | 10 |
| 171 | The microbial degradation of 2,4,6-tribromophenol (TBP) in water/sediments interface: Investigating bioaugmentation using Bacillus sp. GZT. Science of the Total Environment, 2017, 575, 573-580. | 3.9 | 23 |
| 172 | Kinetic and mechanism studies of musk tonalide reacted with hydroxyl radical and the risk assessment of degradation products. Catalysis Today, 2017, 281, 642-648. | 2.2 | 19 |
| 173 | Adsorption Mechanisms of Typical Carbonyl-Containing Volatile Organic Compounds on Anatase TiO ₂ (001) Surface: A DFT Investigation. Journal of Physical Chemistry C, 2017, 121, 13717-13722. | 1.5 | 46 |
| 174 | Photoelectrocatalytic Inactivation Mechanism of Bacteria. Green Chemistry and Sustainable Technology, 2017, , 239-257. | 0.4 | 0 |
| 175 | Indirect photochemical transformations of acyclovir and penciclovir in aquatic environments increase ecological risk. Environmental Toxicology and Chemistry, 2016, 35, 584-592. | 2.2 | 17 |
| 176 | Enhancing tetrabromobisphenol A biodegradation in river sediment microcosms and understanding the corresponding microbial community. Environmental Pollution, 2016, 208, 796-802. | 3.7 | 65 |
| 177 | Controlled growth of CuO/Cu2O hollow microsphere composites as efficient visible-light-active photocatalysts. Applied Catalysis A: General, 2016, 521, 34-41. | 2.2 | 47 |
| 178 | The health risk attenuation by simultaneous elimination of atmospheric VOCs and POPs from an e-waste dismantling workshop by an integrated de-dusting with decontamination technique. Chemical Engineering Journal, 2016, 301, 299-305. | 6.6 | 37 |
| 179 | Bioaccumulation and ecotoxicity increase during indirect photochemical transformation of polycyclic musk tonalide: A modeling study. Water Research, 2016, 105, 47-55. | 5.3 | 43 |
| 180 | Draft Genome Sequence of a Tetrabromobisphenol A–Degrading Strain, <i>Ochrobactrum</i> sp. T, Isolated from an Electronic Waste Recycling Site. Genome Announcements, 2016, 4, . | 0.8 | 3 |

| # | Article | IF | CITATIONS |
|-----|---|------|-----------|
| 181 | Draft Genome Sequence of Bacillus sp. GZT, a 2,4,6-Tribromophenol-Degrading Strain Isolated from the River Sludge of an Electronic Waste-Dismantling Region. Genome Announcements, 2016, 4, . | 0.8 | 0 |
| 182 | Differences in photoelectrocatalytic inactivation processes between E. coli and its isogenic single gene knockoff mutants: Destruction of membrane framework or associated proteins?. Applied Catalysis B: Environmental, 2016, 188, 360-366. | 10.8 | 34 |
| 183 | Enhanced simultaneous PEC eradication of bacteria and antibiotics by facilely fabricated high-activity {001} facets TiO2 mounted onto TiO2 nanotubular photoanode. Water Research, 2016, 101, 597-605. | 5.3 | 46 |
| 184 | Synergistic photocatalytic inactivation mechanisms of bacteria by graphene sheets grafted plasmonic Ag AgX (XÂ=ÂCl, Br, I) composite photocatalyst under visible light irradiation. Water Research, 2016, 99, 149-161. | 5.3 | 122 |
| 185 | Soft-template assisted synthesis of mesoporous CuO/Cu 2 O composite hollow microspheres as efficient visible-light photocatalyst. Materials Letters, 2016, 182, 47-51. | 1.3 | 26 |
| 186 | Emission patterns and risk assessment of polybrominated diphenyl ethers and bromophenols in water and sediments from the Beijiang River, South China. Environmental Pollution, 2016, 219, 596-603. | 3.7 | 57 |
| 187 | The role of catalase and H2O2 in photocatalytic inactivation of Escherichia coli: Genetic and biochemical approaches. Catalysis Today, 2016, 266, 205-211. | 2.2 | 9 |
| 188 | Theoretical investigation on the kinetics and mechanisms of hydroxyl radical-induced transformation of parabens and its consequences for toxicity: Influence of alkyl-chain length. Water Research, 2016, 91, 77-85. | 5.3 | 117 |
| 189 | Unveiling the photoelectrocatalytic inactivation mechanism of Escherichia coli : Convincing evidence from responses of parent and anti-oxidation single gene knockout mutants. Water Research, 2016, 88, 135-143. | 5.3 | 50 |
| 190 | Boron doped BiOBr nanosheets with enhanced photocatalytic inactivation of Escherichia coli. Applied Catalysis B: Environmental, 2016, 192, 35-45. | 10.8 | 213 |
| 191 | Photocatalytic inactivation of Escherichia coli—The roles of genes in β-oxidation of fatty acid degradation. Catalysis Today, 2016, 266, 219-225. | 2.2 | 6 |
| 192 | Comparative elimination of dimethyl disulfide by maifanite and ceramic-packed biotrickling filters and their response to microbial community. Bioresource Technology, 2016, 202, 76-83. | 4.8 | 36 |
| 193 | A novel method developed for estimating mineralization efficiencies and its application in PC and PEC degradations of large molecule biological compounds with unknown chemical formula. Water Research, 2016, 95, 150-158. | 5.3 | 9 |
| 194 | Visible-light-driven photocatalytic bacterial inactivation and the mechanism of zinc oxysulfide under LED light irradiation. Journal of Materials Chemistry A, 2016, 4, 1052-1059. | 5.2 | 60 |
| 195 | VOCs elimination and health risk reduction in e-waste dismantling workshop using integrated techniques of electrostatic precipitation with advanced oxidation technologies. Journal of Hazardous Materials, 2016, 302, 395-403. | 6.5 | 71 |
| 196 | Can environmental pharmaceuticals be photocatalytically degraded and completely mineralized in water using g-C3N4/TiO2 under visible light irradiation?—Implications of persistent toxic intermediates. Applied Catalysis B: Environmental, 2016, 180, 726-732. | 10.8 | 148 |
| 197 | Theoretical investigation on the adsorption configuration and •OH-initiated photocatalytic degradation mechanism of typical atmospheric VOCs styrene onto (TiO2)n clusters. Scientific Reports, 2015, 5, 15059. | 1.6 | 20 |
| 198 | Development of methodology for the determination of carbon isotope ratios using gas chromatography/combustion/isotope ratio mass spectrometry and applications in the biodegradation of phenolic brominated flame retardants and their degradation products. Rapid Communications in Mass Spectrometry, 2015, 29, 54-60. | 0.7 | 7 |

| # | Article | IF | CITATIONS |
|-----|--|------|-----------|
| 199 | Visible-light-driven BiOBr nanosheets for highly facet-dependent photocatalytic inactivation of Escherichia coli. Journal of Materials Chemistry A, 2015, 3, 15148-15155. | 5.2 | 165 |
| 200 | Enhanced visible-light-driven photocatalytic inactivation of Escherichia coli using g-C3N4/TiO2 hybrid photocatalyst synthesized using a hydrothermal-calcination approach. Water Research, 2015, 86, 17-24. | 5.3 | 323 |
| 201 | Dual Roles of Capsular Extracellular Polymeric Substances in Photocatalytic Inactivation of Escherichia coli: Comparison of E. coli BW25113 and Isogenic Mutants. Applied and Environmental Microbiology, 2015, 81, 5174-5183. | 1.4 | 37 |
| 202 | Can Silica Particles Reduce Air Pollution by Facilitating the Reactions of Aliphatic Aldehyde and NO ₂ ?. Journal of Physical Chemistry A, 2015, 119, 11376-11383. | 1.1 | 10 |
| 203 | Theoretical investigation on the role of mineral dust aerosol in atmospheric reaction: A case of the heterogeneous reaction of formaldehyde with NO 2 onto SiO 2 dust surface. Atmospheric Environment, 2015, 103, 207-214. | 1.9 | 18 |
| 204 | Pollution characteristics and health risk assessment of volatile organic compounds emitted from different plastic solid waste recycling workshops. Environment International, 2015, 77, 85-94. | 4.8 | 157 |
| 205 | Efficient bio-deodorization of thioanisole by a novel bacterium Brevibacillus borstelensis GIGAN1 immobilized onto different parking materials in twin biotrickling filter. Bioresource Technology, 2015, 182, 82-88. | 4.8 | 21 |
| 206 | Role of <i>in Situ</i> Resultant H ₂ O ₂ in the Visible-Light-Driven Photocatalytic Inactivation of <i>E. coli</i> Using Natural Sphalerite: A Genetic Study. Journal of Physical Chemistry B, 2015, 119, 3104-3111. | 1.2 | 29 |
| 207 | Cross-linked ZnIn 2 S 4 /rGO composite photocatalyst for sunlight-driven photocatalytic degradation of 4-nitrophenol. Applied Catalysis B: Environmental, 2015, 168-169, 266-273. | 10.8 | 101 |
| 208 | Photocatalytic degradation of three amantadine antiviral drugs as well as their eco-toxicity evolution. Catalysis Today, 2015, 258, 602-609. | 2.2 | 14 |
| 209 | Visible-light-driven inactivation of Escherichia coli K-12 over thermal treated natural pyrrhotite. Applied Catalysis B: Environmental, 2015, 176-177, 749-756. | 10.8 | 50 |
| 210 | Photocatalytic and photoelectrocatalytic degradation and mineralization of small biological compounds amino acids at TiO2 photoanodes. Catalysis Today, 2015, 245, 46-53. | 2.2 | 13 |
| 211 | Thiourea sole doping reagent approach for controllable N, S co-doping of pre-synthesized large-sized carbon nanospheres as electrocatalyst for oxygen reduction reaction. Carbon, 2015, 92, 339-347. | 5.4 | 59 |
| 212 | Simultaneous nutrient removal, optimised CO2 mitigation and biofuel feedstock production by Chlorogonium sp. grown in secondary treated non-sterile saline sewage effluent. Journal of Hazardous Materials, 2015, 297, 241-250. | 6.5 | 13 |
| 213 | The role and synergistic effect of the light irradiation and H2O2 in photocatalytic inactivation of Escherichia coli. Journal of Photochemistry and Photobiology B: Biology, 2015, 149, 164-171. | 1.7 | 22 |
| 214 | Mechanistic study of the visible-light-driven photocatalytic inactivation of bacteria by graphene oxide–zinc oxide composite. Applied Surface Science, 2015, 358, 137-145. | 3.1 | 48 |
| 215 | Eco-toxicity and human estrogenic exposure risks from OH-initiated photochemical transformation of four phthalates in water: A computational study. Environmental Pollution, 2015, 206, 510-517. | 3.7 | 70 |
| 216 | Pollution profiles and risk assessment of PBDEs and phenolic brominated flame retardants in water environments within a typical electronic waste dismantling region. Environmental Geochemistry and Health, 2015, 37, 457-473. | 1.8 | 77 |

| # | Article | IF | CITATIONS |
|-----|--|------|-----------|
| 217 | N-type Cu2O Film for Photocatalytic and Photoelectrocatalytic Processes: Its stability and Inactivation of E. coli. Electrochimica Acta, 2015, 153, 583-593. | 2.6 | 34 |
| 218 | Photocatalytic and photoelectrocatalytic degradation of small biological compounds at TiO2 photoanode: A case study of nucleotide bases. Catalysis Today, 2015, 242, 363-371. | 2.2 | 17 |
| 219 | Aerobic biodegradation of odorous dimethyl disulfide in aqueous medium by isolated Bacillus cereus GIGAN2 and identification of transformation intermediates. Bioresource Technology, 2015, 175, 563-568. | 4.8 | 28 |
| 220 | Theoretical model on the formation possibility of secondary organic aerosol from OH initialed oxidation reaction of styrene in the presence of O 2 /NO. Atmospheric Environment, 2015, 101, 1-9. | 1.9 | 24 |
| 221 | Photocatalytic degradation and mineralization mechanism and toxicity assessment of antivirus drug acyclovir: Experimental and theoretical studies. Applied Catalysis B: Environmental, 2015, 164, 279-287. | 10.8 | 100 |
| 222 | Experimental and theoretical insights into photochemical transformation kinetics and mechanisms of aqueous propylparaben and risk assessment of its degradation products. Environmental Toxicology and Chemistry, 2014, 33, 1809-1816. | 2.2 | 24 |
| 223 | Mechanism, kinetics and toxicity assessment of OH-initiated transformation of triclosan in aquatic environments. Water Research, 2014, 49, 360-370. | 5.3 | 161 |
| 224 | Synthesis and characterization of N-doped carbonaceous/TiO2 composite photoanodes for visible-light photoelectrocatalytic inactivation of Escherichia coli K-12. Catalysis Today, 2014, 230, 67-73. | 2.2 | 29 |
| 225 | Visible-light-driven photocatalytic inactivation of E. coli by Ag/AgX-CNTs (X=Cl, Br, I) plasmonic photocatalysts: Bacterial performance and deactivation mechanism. Applied Catalysis B: Environmental, 2014, 158-159, 301-307. | 10.8 | 149 |
| 226 | UV and visible light photoelectrocatalytic bactericidal performance of 100% {111} faceted rutile TiO2 photoanode. Catalysis Today, 2014, 224, 77-82. | 2.2 | 30 |
| 227 | Systematic Approach to In-Depth Understanding of Photoelectrocatalytic Bacterial Inactivation Mechanisms by Tracking the Decomposed Building Blocks. Environmental Science & Technology, 2014, 48, 9412-9419. | 4.6 | 169 |
| 228 | Anatase TiO2 nanoparticles–carbon nanotubes composite: Optimization synthesis and the relationship of photocatalytic degradation activity of acyclovir in water. Applied Catalysis A: General, 2014, 485, 188-195. | 2.2 | 24 |
| 229 | Pollution profiles and health risk assessment of VOCs emitted during e-waste dismantling processes associated with different dismantling methods. Environment International, 2014, 73, 186-194. | 4.8 | 140 |
| 230 | Concurrent degradation of tetrabromobisphenol A by Ochrobactrum sp. T under aerobic condition and estrogenic transition during these processes. Ecotoxicology and Environmental Safety, 2014, 104, 220-225. | 2.9 | 32 |
| 231 | Distribution, possible sources, and health risk assessment of SVOC pollution in small streams in Pearl River Delta, China. Environmental Science and Pollution Research, 2014, 21, 10083-10095. | 2.7 | 30 |
| 232 | Kinetics and Mechanism of [•] OH Mediated Degradation of Dimethyl Phthalate in Aqueous Solution: Experimental and Theoretical Studies. Environmental Science & Technology, 2014, 48, 641-648. | 4.6 | 144 |
| 233 | Anatase TiO2 mesocrystals with exposed (001) surface for enhanced photocatalytic decomposition capability toward gaseous styrene. Catalysis Today, 2014, 224, 216-224. | 2.2 | 38 |
| 234 | Comparative study on the photoelectrocatalytic inactivation of Escherichia coli K-12 and its mutant Escherichia coli BW25113 using TiO2 nanotubes as a photoanode. Applied Catalysis B: Environmental, 2014, 147, 562-570. | 10.8 | 54 |

| # | Article | IF | CITATIONS |
|-----|---|------|-----------|
| 235 | Vapor-phase hydrothermal synthesis of rutile TiO2 nanostructured film with exposed pyramid-shaped (1 1 1) surface and superiorly photoelectrocatalytic performance. Journal of Colloid and Interface Science, 2014, 429, 53-61. | 5.0 | 24 |
| 236 | Computational consideration on advanced oxidation degradation of phenolic preservative, methylparaben, in water: mechanisms, kinetics, and toxicity assessments. Journal of Hazardous Materials, 2014, 278, 417-425. | 6.5 | 69 |
| 237 | Adenovirus inactivation by in situ photocatalytically and photoelectrocatalytically generated halogen viricides. Chemical Engineering Journal, 2014, 253, 538-543. | 6.6 | 20 |
| 238 | A Recyclable Mineral Catalyst for Visible-Light-Driven Photocatalytic Inactivation of Bacteria: Natural Magnetic Sphalerite. Environmental Science & Technology, 2013, 47, 11166-11173. | 4.6 | 108 |
| 239 | Pollution profiles, health risk of VOCs and biohazards emitted from municipal solid waste transfer station and elimination by an integrated biological-photocatalytic flow system: A pilot-scale investigation. Journal of Hazardous Materials, 2013, 250-251, 147-154. | 6.5 | 83 |
| 240 | Synthesis and Characterization of Novel Plasmonic Ag/AgX-CNTs (X = Cl, Br, I) Nanocomposite Photocatalysts and Synergetic Degradation of Organic Pollutant under Visible Light. ACS Applied Materials & Interfaces, 2013, 5, 6959-6967. | 4.0 | 144 |
| 241 | Comparative study of visible-light-driven photocatalytic inactivation of two different wastewater bacteria by natural sphalerite. Chemical Engineering Journal, 2013, 234, 43-48. | 6.6 | 34 |
| 242 | Photocatalytic and photoelectrocatalytic degradation of small biological compounds: A case study of uridine. Catalysis Today, 2013, 201, 167-174. | 2.2 | 10 |
| 243 | CdIn2S4 microsphere as an efficient visible-light-driven photocatalyst for bacterial inactivation: Synthesis, characterizations and photocatalytic inactivation mechanisms. Applied Catalysis B: Environmental, 2013, 129, 482-490. | 10.8 | 170 |
| 244 | Synthesis of TiO2 hollow sphere multimer photocatalyst by etching titanium plate and its application to the photocatalytic decomposition of gaseous styrene. Chemical Engineering Journal, 2013, 228, 834-842. | 6.6 | 38 |
| 245 | Kinetic optimization of biodegradation and debromination of 2,4,6-tribromophenol using response surface methodology. International Biodeterioration and Biodegradation, 2013, 76, 18-23. | 1.9 | 18 |
| 246 | Comparative studies of photocatalytic and photoelectrocatalytic inactivation of E. coli in presence of halides. Applied Catalysis B: Environmental, 2013, 140-141, 225-232. | 10.8 | 37 |
| 247 | Advanced Oxidation Kinetics and Mechanism of Preservative Propylparaben Degradation in Aqueous Suspension of TiO ₂ and Risk Assessment of Its Degradation Products. Environmental Science & Technology, 2013, 47, 2704-2712. | 4.6 | 161 |
| 248 | Distribution profile, health risk and elimination of model atmospheric SVOCs associated with a typical municipal garbage compressing station in Guangzhou, South China. Atmospheric Environment, 2013, 76, 173-180. | 1.9 | 19 |
| 249 | Instant inactivation and rapid decomposition of Escherichia coli using a high efficiency TiO2 nanotube array photoelectrode. RSC Advances, 2013, 3, 20824. | 1.7 | 11 |
| 250 | Synthesis and characterization of <scp>TiO₂</scp> nanotube photoanode and its application in photoelectrocatalytic degradation of model environmental pharmaceuticals. Journal of Chemical Technology and Biotechnology, 2013, 88, 1488-1497. | 1.6 | 46 |
| 251 | A theoretical model on the formation mechanism and kinetics of highly toxic air pollutants from halogenated formaldehydes reacted with halogen atoms. Atmospheric Chemistry and Physics, 2013, 13, 11277-11286. | 1.9 | 28 |
| 252 | Determination of chemical oxygen demand of nitrogenous organic compounds in wastewater using synergetic photoelectrocatalytic oxidation effect at TiO2 nanostructured electrode. Analytica Chimica Acta, 2012, 754, 47-53. | 2.6 | 32 |

| # | Article | IF | CITATIONS |
|-----|---|------|-----------|
| 253 | Synthesis of Carbon Nanotube–Anatase TiO ₂ Sub-micrometer-sized Sphere Composite Photocatalyst for Synergistic Degradation of Gaseous Styrene. ACS Applied Materials & Interfaces, 2012, 4, 5988-5996. | 4.0 | 128 |
| 254 | Visible-Light-Driven Photocatalytic Inactivation of <i>E. coli</i> K-12 by Bismuth Vanadate Nanotubes: Bactericidal Performance and Mechanism. Environmental Science & Technology, 2012, 46, 4599-4606. | 4.6 | 254 |
| 255 | Genetic studies of the role of fatty acid and coenzyme A in photocatalytic inactivation of Escherichia coli. Water Research, 2012, 46, 3951-3957. | 5.3 | 35 |
| 256 | Treatment of organic waste gas in a paint plant by combined technique of biotrickling filtration with photocatalytic oxidation. Chemical Engineering Journal, 2012, 200-202, 645-653. | 6.6 | 45 |
| 257 | Efficient bio-deodorization of aniline vapor in a biotrickling filter: Metabolic mineralization and bacterial community analysis. Chemosphere, 2012, 87, 253-258. | 4.2 | 17 |
| 258 | Optimization synthesis of carbon nanotubes-anatase TiO2 composite photocatalyst by response surface methodology for photocatalytic degradation of gaseous styrene. Applied Catalysis B: Environmental, 2012, 123-124, 69-77. | 10.8 | 102 |
| 259 | Theoretical study of the reaction mechanism and kinetics of low-molecular-weight atmospheric aldehydes (C1–C4) with NO2. Atmospheric Environment, 2012, 54, 288-295. | 1.9 | 30 |
| 260 | Biodegradation kinetics and mechanism of 2,4,6-tribromophenol by Bacillus sp. GZT: A phenomenon of xenobiotic methylation during debromination. Bioresource Technology, 2012, 110, 153-159. | 4.8 | 34 |
| 261 | Biodegradation and detoxification of bisphenol A with one newly-isolated strain Bacillus sp. GZB: Kinetics, mechanism and estrogenic transition. Bioresource Technology, 2012, 114, 224-230. | 4.8 | 94 |
| 262 | Distribution, sources, and potential toxicological significance of PAHs in drinking water sources within the Pearl River Delta. Journal of Environmental Monitoring, 2011, 13, 1457. | 2.1 | 25 |
| 263 | Structural Characterization and Photocatalytic Activity of Hydrothermally Synthesized Mesoporous TiO2 for 2,4,6-Tribromophenol Degradation in Water. Chinese Journal of Catalysis, 2011, 32, 1349-1356. | 6.9 | 5 |
| 264 | Photocatalytic degradation kinetics and mechanism of antivirus drug-lamivudine in TiO2 dispersion. Journal of Hazardous Materials, 2011, 197, 229-236. | 6.5 | 141 |
| 265 | In situ photoelectrocatalytic generation of bactericide for instant inactivation and rapid decomposition of Gram-negative bacteria. Journal of Catalysis, 2011, 277, 88-94. | 3.1 | 65 |
| 266 | On-site and off-site atmospheric PBDEs in an electronic dismantling workshop in south China: Gas-particle partitioning and human exposure assessment. Environmental Pollution, 2011, 159, 3529-3535. | 3.7 | 60 |
| 267 | Comparative study of visible-light-driven photocatalytic mechanisms of dye decolorization and bacterial disinfection by B–Ni-codoped TiO2 microspheres: The role of different reactive species. Applied Catalysis B: Environmental, 2011, 108-109, 108-116. | 10.8 | 158 |
| 268 | One-step process for debromination and aerobic mineralization of tetrabromobisphenol-A by a novel Ochrobactrum sp. T isolated from an e-waste recycling site. Bioresource Technology, 2011, 102, 9148-9154. | 4.8 | 107 |
| 269 | Assessment of typical pollutants in waterborne by combining active biomonitoring and integrated biomarkers response. Chemosphere, 2011, 84, 1422-1431. | 4.2 | 33 |
| 270 | Photocatalytic inactivation of Escherichia coli by natural sphalerite suspension: Effect of spectrum, wavelength and intensity of visible light. Chemosphere, 2011, 84, 1276-1281. | 4.2 | 28 |

| # | Article | IF | CITATIONS |
|-----|--|------|-----------|
| 271 | Purification of waste gas containing high concentration trimethylamine in biotrickling filter inoculated with B350 mixed microorganisms. Bioresource Technology, 2011, 102, 6757-6760. | 4.8 | 33 |
| 272 | Treatment performance of volatile organic sulfide compounds by the immobilized microorganisms of B350 group in a biotrickling filter. Journal of Chemical Technology and Biotechnology, 2011, 86, 1166-1176. | 1.6 | 10 |
| 273 | Synthesis and characterization of novel SiO2 and TiO2 co-pillared montmorillonite composite for adsorption and photocatalytic degradation of hydrophobic organic pollutants in water. Catalysis Today, 2011, 164, 364-369. | 2.2 | 43 |
| 274 | Photocatalytic degradation and detoxification of o-chloroaniline in the gas phase: Mechanistic consideration and mutagenicity assessment of its decomposed gaseous intermediate mixture. Applied Catalysis B: Environmental, 2011, 102, 140-146. | 10.8 | 43 |
| 275 | Co-treatment of single, binary and ternary mixture gas of ethanethiol, dimethyl disulfide and thioanisole in a biotrickling filter seeded with Lysinibacillus sphaericus RG-1. Journal of Hazardous Materials, 2011, 186, 1050-1057. | 6.5 | 33 |
| 276 | Adsorption and degradation of model volatile organic compounds by a combined titania–montmorillonite–silica photocatalyst. Journal of Hazardous Materials, 2011, 190, 416-423. | 6.5 | 85 |
| 277 | Photocatalytic degradation kinetics and mechanism of environmental pharmaceuticals in aqueous suspension of TiO2: A case of β-blockers. Journal of Hazardous Materials, 2010, 179, 834-839. | 6.5 | 171 |
| 278 | Biodegradation of ethanethiol in aqueous medium by a new Lysinibacillus sphaericus strain RG-1 isolated from activated sludge. Biodegradation, 2010, 21, 1057-1066. | 1.5 | 44 |
| 279 | Synthesis and characterization of novel magnetic Fe3O4/polyurethane foam composite applied to the carrier of immobilized microorganisms for wastewater treatment. Research on Chemical Intermediates, 2010, 36, 277-288. | 1.3 | 58 |
| 280 | Comparison of the removal of ethanethiol in twin-biotrickling filters inoculated with strain RG-1 and B350 mixed microorganisms. Journal of Hazardous Materials, 2010, 183, 372-380. | 6.5 | 46 |
| 281 | Gas-phase photocatalytic degradation and detoxification of o-toluidine: Degradation mechanism and Salmonella mutagenicity assessment of mixed gaseous intermediates. Journal of Molecular Catalysis A, 2010, 333, 128-135. | 4.8 | 16 |
| 282 | Preparation, characterisation and sensing application of inkjet-printed nanostructured TiO2 photoanode. Sensors and Actuators B: Chemical, 2010, 147, 622-628. | 4.0 | 33 |
| 283 | Kinetics and mechanism of advanced oxidation processes (AOPs) in degradation of ciprofloxacin in water. Applied Catalysis B: Environmental, 2010, 94, 288-294. | 10.8 | 486 |
| 284 | Photocatalytic degradation kinetics and mechanism of environmental pharmaceuticals in aqueous suspension of TiO2: A case of sulfa drugs. Catalysis Today, 2010, 153, 200-207. | 2.2 | 171 |
| 285 | The fabrication of CNTs/TiO2photoanodes for sensitive determination of organic compounds. Nanotechnology, 2010, 21, 485503. | 1.3 | 12 |
| 286 | Mechanistic Considerations for the Advanced Oxidation Treatment of Fluoroquinolone Pharmaceutical Compounds using TiO ₂ Heterogeneous Catalysis. Journal of Physical Chemistry A, 2010, 114, 2569-2575. | 1.1 | 160 |
| 287 | Mechanistic study and mutagenicity assessment of intermediates in photocatalytic degradation of gaseous toluene. Chemosphere, 2010, 78, 313-318. | 4.2 | 40 |
| 288 | Safety assessment of the source water within the Pearl River Delta on the aspect of organochlorine pesticides contamination. Journal of Environmental Monitoring, 2010, 12, 1666. | 2.1 | 26 |

| # | Article | IF | CITATIONS |
|-----|--|-----|-----------|
| 289 | Direct growth of hierarchically structured titanate nanotube filtration membrane for removal of waterborne pathogens. Journal of Membrane Science, 2009, 343, 212-218. | 4.1 | 23 |
| 290 | Degradation of toluene gas at the surface of ZnO/SnO2 photocatalysts in a baffled bed reactor. Research on Chemical Intermediates, 2009, 35, 827-838. | 1.3 | 12 |
| 291 | Preparation and characterization of highly active mesoporous TiO2 photocatalysts by hydrothermal synthesis under weak acid conditions. Microporous and Mesoporous Materials, 2009, 124, 197-203. | 2.2 | 84 |
| 292 | A portable miniature UV-LED-based photoelectrochemical system for determination of chemical oxygen demand in wastewater. Sensors and Actuators B: Chemical, 2009, 141, 634-640. | 4.0 | 64 |
| 293 | Comparative study of the eliminating of waste gas containing toluene in twin biotrickling filters packed with molecular sieve and polyurethane foam. Journal of Hazardous Materials, 2009, 167, 275-281. | 6.5 | 40 |
| 294 | Effect of synthesis conditions on photocatalytic activities of nanoparticulate TiO2 thin films. Separation and Purification Technology, 2009, 68, 83-89. | 3.9 | 28 |
| 295 | Photocatalytic degradation of dimethyl phthalate ester using novel hydrophobic TiO2 pillared montmorillonite photocatalyst. Research on Chemical Intermediates, 2008, 34, 67-83. | 1.3 | 39 |
| 296 | Comparative study of the elimination of toluene vapours in twin biotrickling filters using two microorganismsBacillus cereus S1 and S2. Journal of Chemical Technology and Biotechnology, 2008, 83, 1019-1026. | 1.6 | 33 |
| 297 | Preparation and characterization of hydrophobic TiO2 pillared clay: The effect of acid hydrolysis catalyst and doped Pt amount on photocatalytic activity. Journal of Colloid and Interface Science, 2008, 320, 501-507. | 5.0 | 63 |
| 298 | Structural and photocatalytic degradation characteristics of hydrothermally treated mesoporous TiO2. Applied Catalysis A: General, 2008, 350, 237-243. | 2.2 | 81 |
| 299 | Characterization and the photocatalytic activity of TiO2 immobilized hydrophobic montmorillonite photocatalysts. Catalysis Today, 2008, 139, 69-76. | 2.2 | 117 |
| 300 | Recent Patents on Immobilized Microorganism Technology and Its Engineering Application in Wastewater Treatment. Recent Patents on Engineering, 2008, 2, 28-35. | 0.3 | 50 |
| 301 | MUTAGENICITY ASSESSMENT OF PRODUCED WATER DURING PHOTOELECTROCATALYTIC DEGRADATION. Environmental Toxicology and Chemistry, 2007, 26, 416. | 2.2 | 33 |
| 302 | Improving ultraviolet light transmission in a packed-bed photoelectrocatalytic reactor for removal of oxalic acid from wastewater. Journal of Photochemistry and Photobiology A: Chemistry, 2006, 181, 158-165. | 2.0 | 15 |
| 303 | Photoelectrocatalytic decontamination of oilfield produced wastewater containing refractory organic pollutants in the presence of high concentration of chloride ions. Journal of Hazardous Materials, 2006, 138, 392-400. | 6.5 | 115 |
| 304 | Photoelectrocatalytic degradation of oxalic acid in aqueous phase with a novel three-dimensional electrode-hollow quartz tube photoelectrocatalytic reactor. Applied Catalysis A: General, 2005, 279, 247-256. | 2.2 | 39 |
| 305 | Insect resistance toNilaparvata lugens andCnaphalocrocis medinalis in transgenic indica rice and the inheritance ofgna+sbti transgenes. Pest Management Science, 2005, 61, 390-396. | 1.7 | 23 |
| 306 | Synergetic effect in degradation of formic acid using a new photoelectrochemical reactor. Journal of Photochemistry and Photobiology A: Chemistry, 2002, 152, 155-165. | 2.0 | 65 |